



Published in final edited form as:

Behav Brain Res. 2011 January 20; 216(2): 543–551. doi:10.1016/j.bbr.2010.08.036.

Stress-Induced Changes In C-Fos And Corticotropin Releasing Hormone Immunoreactivity In The Amygdala Of The Spontaneously Hypertensive Rat

Karen Porter and Linda F Hayward

Abstract

The present study was undertaken to test the hypothesis that dysregulation of the amygdala contributes to the exaggerated autonomic response to stress in an animal model of essential hypertension. Spontaneously hypertensive (SHR) and normotensive Wistar male rats were chronically instrumented and exposed to 20 min of either air jet stress (AJS) or air noise alone (CON). AJS induced a significant increase in both heart rate and arterial pressure that was greater in the SHR. AJS induced a significant increase in c-Fos-like immunoreactivity (FLI) throughout the caudal-rostral extent of the basolateral, medial, and central (CEA) subnuclei of the amygdala. Differences in FLI between strains were localized to the rostral CEA and the SHR expressed significantly less FLI. AJS also induced a significant increase in the number of corticotrophin releasing hormone (CRH) positive neurons in the CEA. Differences between strains were localized to the caudal CEA and the number of CRH-positive cells was significantly greater in the SHR. The stress-induced increase in CRH-labeling in caudal CEA of the SHR was coupled to a greater increase in FLI in the rostral locus coeruleus (LC) of the SHR versus the Wistar. AJS also induced significant increases in FLI in several hypothalamus subnuclei, but no strain-related differences were identified. These results suggest for the first time that dysregulation of CRH-positive cells in the caudal CEA and reduced excitation and/or exaggerated inhibition of rostral CEA neurons may contribute to the exaggerated cardiovascular response to stress in the SHR, possibly through descending modulation of the rostral LC.

Keywords

Stress; Hypertension; Amygdala; Hypothalamus; Locus Coeruleus; c-Fos

INTRODUCTION

Individuals with hypertension often elicit exaggerated cardiovascular, hormonal, and behavioral responses to stress (1,27). In humans, feelings of anxiety or fear have been associated with activation of the amygdala. The amygdala is a complex structure in the forebrain that has been linked to modulation of autonomic, neuroendocrine, and behavioral responses to different types of stress, including internal stressors, such as hypotension or inflammation, and external stressors, like physical restraint or fearful social contexts (12,15,16,58,59). Autonomic and emotional responses to stressful situations have been reported to be attenuated in individuals with lesions of the amygdala (2,62,74).

© 2010 Elsevier B.V. All rights reserved.

Publisher's Disclaimer: This is a PDF file of an unedited manuscript that has been accepted for publication. As a service to our customers we are providing this early version of the manuscript. The manuscript will undergo copyediting, typesetting, and review of the resulting proof before it is published in its final citable form. Please note that during the production process errors may be discovered which could affect the content, and all legal disclaimers that apply to the journal pertain.

Alternatively, individuals with exaggerated cardiovascular responses to stressful stimuli show evidence of increased neuronal excitation within the amygdala which is correlated with a predisposition for high blood pressure (25). As a result, it has been hypothesized that dysregulation of the amygdala may predispose an individual to develop hypertension (36).

Three main subnuclei encompass the amygdala, including the lateral and basolateral complex (BLA), the central nucleus (CEA) and the medial nucleus (MEA) of the amygdala (40). In general, the BLA complex is thought to function as an integrator of incoming sensory input and via an interneuronal system this subnucleus acts to modulate neuronal excitation within the CEA (40). The CEA, in turn, sends projections to many important nuclei throughout the brain, including the hypothalamus, locus coeruleus, parabrachial nucleus, and periaqueductal gray (14,26,57,70,71), coordinating autonomic and behavioral responses to stress. Finally, the MEA interconnects with both the BLA and CEA, but has primarily been implicated in modulating the hypothalamic-pituitary-adrenal (HPA) axis (42). Based on the high concentration of inhibitory interneurons within the amygdala, it has been proposed that activation of the BLA by fearful or stressful stimuli may functionally inhibit CEA and MEA inhibitory projection neurons, thereby disinhibiting distal target sites (51,53). Yet, the exact conditions under which the CEA and MEA projection neurons are excited or inhibited remain to be fully elucidated. Furthermore, many of the neurotransmitters, such as corticotrophin releasing hormone (CRH), which can be found in high concentrations within the amygdala, are known to have a powerful impact on neuronal processing during stress (58,65). Yet, the role of these peptides in exaggerated stress responses elicited in hypertensive individuals remains to be defined.

To date several lesion studies have exposed a role for the CEA (21,24) and the MEA (23) in mediating augmented responses to stressful stimuli and the development of high blood pressure in an animal model of essential hypertension, the spontaneously hypertensive rat (SHR). Since the MEA and CEA are interconnected either directly or indirectly via feedback from the HPA axis (27-29), the exact site for stress-related dysfunction within the amygdala in this animal model remains to be identified. Indeed, to our knowledge no previous studies have examined the pattern of neuronal activation within the amygdala of the SHR following exposure to acute stress. Prior studies have only examined changes in c-Fos, an early marker of neuronal activation, in the brainstem and the hypothalamus after acute stress in the SHR versus normotensive rats (34,50). In those regions, some significant differences between strains were identified; suggesting that strain related differences may also exist in the amygdala. Furthermore, since CRH release from the CEA may modulate the response to stress (12,43,58), it is surprising that the response of CRH neurons within the amygdala of the SHR has also not been previously examined. Indeed, evidence indicating an alteration in the regulation of CRH in other brain regions in the SHR raises the possibility that dysregulation of CRH neurons within the amygdala could also contribute to exaggerated responses to fearful stimuli in this hypertensive strain (28,30,38).

Due to the limited information describing how the different subnuclei of the amygdala respond to acute stress in the SHR, the following investigation was undertaken to test the hypothesis that both the CEA and the MEA of the SHR would demonstrate altered neuronal responses to stress when compared to a normotensive strain.

MATERIALS AND METHODS

General Preparation

All experimental procedures were approved by the University of Florida Institutional Animal Care and Use Committee and followed the NIH guidelines. Male SHR and normotensive Wistar rats (10-12 weeks old; Charles River Laboratories, Wilmington, MA)

were randomly assigned to one of two groups: air jet stress (AJS; n=14) or control (CON; n=10). Animals were given a subcutaneous injection of Rimadyl (0.1 mg/kg, Pfizer Animal Health, Exton, MD) and buprenorphine (0.05 mg/kg, Rickett Benckiser Pharmaceuticals, Inc., Richmond, VA) 20 min prior to the induction of anesthesia. Animals were anesthetized to a surgical level (2-4% isoflurane in 100% O₂) and an incision was made on the ventral surface of the hind-limb. Fat, nerves, and connective tissue were gently dissected from the femoral vasculature and catheters (Braintree Scientific, Braintree, MA) directed toward the abdominal aorta were placed into both the femoral artery and vein. Catheters were filled with heparinized saline (100 IU/ml), plugged with obturators, and tunneled subcutaneously to the nape of the neck, exiting between the scapulae, and secured in place with sutures. All incisions were treated with triple antibiotic ointment (Alpharma USPD, Inc., Baltimore, MD) and the animals received a subcutaneous injection of saline (2-3 ml) for fluid replacement and were allowed to recover on a heating pad. An additional injection of buprenorphine (0.02-0.05 mg/kg) was given before returning the animal to its home cage.

All animals were housed individually following surgery and were allowed 48 hours to recover prior to experimentation. On the first day following surgery the animals were brought to the lab, weighed, handled, and acclimated to the experimental container. The acclimation period for all animals included a 50-60 min period of exposure to air noise (~75-80 decibels) while resting in the experimental chamber. Following the acclimation period, animals were returned to their home cages.

Experimental Protocol

All experiments took place between 8:00 AM and 1 PM. On the day of the experiment, the exteriorized catheters were unplugged and connected to PE 50 tubing containing heparinized saline (100 IU/ml). The animals were placed into the experimental chamber (Instech Laboratories, Inc., Plymouth, MA) and the arterial catheter was connected to a calibrated pressure transducer (Stoelting Inc., Wood Dale, IL) for continuous measurement of pulsatile and mean arterial pressure (AP). The experimental chamber consisted of a circular container (15 cm radius) with three tubes (~0.5 cm diameter) inserted into the wall of the chamber, one tube every ~30 cm (equidistance around the circumference) at a height of approximately ~5 cm from the bottom of the chamber. The tubes were connected to a three-way valve manifold for regulation of the air stream through each tube.

At the beginning of the experiment both AJS and CON groups were exposed to a 90 min baseline period of air noise (noise associated with 20 psi room air released from tubing outside of the experimental chamber). For the AJS group, after 90 min of air noise, the pressurized air was switched from being directed away from the chamber to being directed into the chamber through one of three inflow tubes. The AJS protocol was separated into two distinct periods: an initial 5 min period of random AJS (continuous stream of air entering the chamber from random directions and at random durations) followed immediately by a 15 min period of controlled AJS (the direction of the air flow was changed randomly every min). For the CON group, the air noise was continued for another 20 min following the baseline period. After the 20 min of AJS or a comparable noise control period, the pressurized air was turned off and the rats were allowed to recover undisturbed for 90 min. At the termination of the experiment, all animals were deeply anesthetized with sodium pentobarbital (80-100 mg/kg, i.v.) and transcardially perfused with heparinized saline followed by 4% paraformaldehyde in 0.1 M phosphate buffer (pH=7.2). Brains were removed and soaked in 4% paraformaldehyde overnight followed by submersion in a 30% sucrose solution for 48-72 hours. Prior to processing, a small cut was made along the rostral-caudal extent of the right ventral surface of the brain to distinguish left and right sides. Next, the tissue was frozen and sectioned (40 µm coronal slices).

Immunohistochemistry

The sectioned tissue was soaked in phosphate buffered saline (PBS) for approximately 24 hours and then washed in 3% donkey serum and 0.4% Triton X in PBS (3% DS-T-PBS) for one hour. The tissue was incubated overnight in rabbit anti-c-Fos antibody (1:2000 dilution, Santa Cruz Biotechnology, Santa Cruz, CA) diluted with 1% DS-T-PBS. The next day the tissue was washed in 1% DS-T-PBS for one hour, incubated in donkey-anti-rabbit biotinylated immunoglobulin G (Ig) antibody (1:500; Jackson Immuno Research, West Grove, PA) for two hours, and then re-rinsed for 1 hour. The tissue was then incubated for 30 min in an avidin biotinylated-peroxidase tertiary molecule solution (ABC Vectastain Kit, Vector Labs, Burlingame, CA). Following a final wash in 1% DS-T-PBS, the tissue was stained with Vector SC according to manufacturer's instructions (Vector Labs) revealing the c-Fos-like immunoreactivity (FLI) as gray/blue stain in the nucleus of the cell. The brain tissue was then washed 1% DS-T-PBS (3×5 min) re-incubated in 3% DS-T-PBS for one hour, followed by incubation in guinea pig anti-CRH (1:10,000; Peninsula Laboratories, Inc., San Carlos, CA) for 12-24 hours (44). The tissue was rinsed in 1% DS-T-PBS for one hour, incubated with donkey anti-guinea pig biotinylated Ig antibody (1:500; Jackson ImmunoResearch) for two hours, re-rinsed for 1 hour, and then incubated for 30 min in ABC solution, followed by a 1% DS-T-PBS rinse. Finally, the tissue was stained with 0.05% diaminobensidine hydrochloride (DAB, Vector Labs) diluted in 2.5% ammonium sulfate and H₂O₂ in 0.05 M Tris-HCL. Tissue was rinsed three times in PBS and mounted on slides and dried. Slides were dehydrated and coverslipped.

Previous reports have demonstrated that pre-incubation of brain tissue with 20 μ M of CRH peptide eliminates all staining specific to the CRH antibody utilized in this study (4). In the present study, additional negative controls (tissue processed in the absence of the primary antibody) for both CRH- and c-FOS were performed on tissue samples from both strains. In the absence of the primary antibodies, no CRH or c-fos staining was identified.

Data analysis

For the cardiovascular data, heart rate (HR) was derived from the interval between successive systolic peaks of pulsatile AP. Three time periods were analyzed, including baseline, the treatment period (AJS or CON), and recovery. The baseline period was defined as a 2 min average approximately 20 min prior to the treatment period when mean (MAP) and HR remained steady for 5 min. During the treatment period, MAP and HR were averaged over successive two min intervals following the onset of the treatment. Two recovery time points, at 30 and 60 min from the onset of the treatment period were also measured over 2 min blocks. The change from baseline (Δ) in MAP and HR was then calculated for each animal. In addition, the area under the curve (AUC) was quantified during the 20 min treatment period for both Δ MAP and Δ HR (average Δ MAP or HR \times time) to generate a single value during the treatment period per animal.

For immunohistochemical analysis, two slices per animal were imaged for each of the following brain regions: rostral, middle, and caudal amygdala, rostral and caudal LC, the arcuate nucleus (ARC), PVN, and dorsal medial hypothalamus (DMH). Brain regions were identified by anatomical landmarks, such as fiber tracks and surface indentations, defined by the Rat Stereotaxic Atlas (54). For the amygdala, the rostral extent was -1.6 to -2.1 mm, the middle extent was -2.2 to -2.6 mm, and the caudal extent was -2.7 to -3.2 mm caudal to bregma. The rostral and caudal regions of the LC were defined as -9.3 to -9.7 mm and -9.8 to -10.2 mm caudal to bregma, respectively. The ARC was identified between -3.1 and -3.3 mm caudal to bregma. The magnocellular (mPVN) and parvocellular (pPVN) subnuclei of the PVN were identified between -1.7 and -1.9 mm caudal to bregma. Finally, the DMH was located between -2.8 and -3.1 mm caudal to bregma.

Each brain region was imaged at 10-20x (Zeiss Axioskop; Axiovision software), imported into Adobe Photoshop 7.0 and selected subnuclei were fit with a “mask” for cell counting. “Masks” were standardized between animals by regional landmarks. All cell counts were made from the left side of the brain. The criterion for FLI positive neurons was defined by the presence of gray/blue stain localized within the cell's nucleus. CRH-positive cells were identified by a brown color filling the cytosol and the axonal and dendritic processes of the neuron. Cells were counted manually by an individual blinded to the treatment group. Cell counts from the two slices of the same region were averaged to generate a single value per region per animal.

The pattern of staining for CRH-positive neurons in the CEA was similar to previous reports (4,44), including the relative absence of CRH-positive cell bodies in the rostral portion of the CEA and the relative small number of positively CRH-stained neurons in the CON animals (10-20 neurons/slice)(44). As a consequence, no CRH counts were obtained from the rostral CEA. Furthermore, consistent with the observations of other investigators (16) no cells were identified to co-label for both FLI and CRH in the CEA, thus co-labeling was not quantified.

Statistical Analysis

All data are represented as mean±SEM. Cardiovascular data were analyzed using a three-way analysis of the variance (ANOVA) with repeated measures comparing treatment groups and strains against the designated time points (STATVIEW) In the absence of a time effect, a two-way ANOVA comparing treatment and strain using the average Δ MAP or Δ HR over time (AUC) value was used. The treatment and recovery periods were analyzed separately. A two-way ANOVA was also used for comparing strain and treatment effects on immunohistochemical data. For all analyses, when permitted post hoc comparisons were made using either a Scheffe post hoc test or when multiple comparisons were permitted, repeated unpaired t-tests were used with an adjustment of the significance level by the Bonferroni test for multiple comparisons. Statistical significance was set at $P < 0.05$.

RESULTS

Cardiovascular response to air jet stress

Prior to the onset of the treatment, during the 90 min air noise baseline period, MAP of the SHR was significantly higher compared to the Wistar (162 ± 3 vs. 115 ± 2 mmHg, respectively; [$F(1,23)=137.58$]; $P < 0.001$) and baseline HR of the SHRs was significantly lower compared to the Wistars (350 ± 7 vs. 385 ± 13 beats/min, respectively; [$F(1,23)=5.47$]; $P < 0.01$).

Figure 1 illustrates the typical cardiovascular response before, during, and immediately following AJS for each rat strain. At the onset of AJS, AP increased in both strains; however the increase was greater in the SHR. HR also increased rapidly at the onset of AJS and the initial rise from baseline was greater in the SHR. Furthermore, as AJS continued, HR in the Wistar rat gradually began to fall (Fig. 1A), followed by a slight rise at the end of AJS. In contrast, during sustained AJS, HR in the SHR remained steady with only a slight decrease near the end of the stress period (Fig. 1B). At the offset of AJS, MAP and HR gradually returned to baseline in both strains.

Figure 2A demonstrates the average change from baseline for MAP and HR during the 20 min of AJS, the corresponding control period, and during the recovery. During the treatment period a three-way ANOVA of the change in MAP from baseline (Δ MAP) identified a significant interaction between strain and treatment [$F(3,23)=10.8$], but the effect of time was not significant [$F(4,76)=0.77$]. For subsequent analysis, the average Δ MAP was

calculated over the 20 min treatment period (AUC) and a two-way ANOVA identified a significant interaction between strain \times treatment ($[F(3,23)=10.83]$; $P<0.004$). Further analysis identified that the average Δ MAP in the SHR during AJS (SHR-AJS, $n=7$; see Figure 2B) was significantly greater than the average Δ MAP elicited in the Wistar during AJS (W-AJS, $n=7$; $[F(1,13)=31.11]$; $P=0.0001$) and both CON groups ($n=5$ /group; $[F(1,11)>26.5]$; $P<0.0005$). The average Δ MAP in the W-AJS group, however, was not significantly different from either CON group ($[F(1,11)<1.85]$; $P>0.15$). Comparisons between the CON groups did not demonstrate any difference in average Δ MAP between strains during the treatment period $[F(1,9)=0.45]$. Recovery points for all groups were not significantly different from each other.

Statistical analysis of the change in HR (Δ HR) from baseline during the treatment period also did not identify a significant effect of time $[F(4,76)=0.48]$, however there was a significant interaction between strain and treatment ($[F(3,23)=5.3]$; $P=0.02$). Subsequent analysis of the average Δ HR during the 20 min treatment period (AUC; bottom Figure 2B) identified a significant strain \times treatment interaction $[F(3,23)=5.34]$ and the average Δ HR of the SHR-AJS group was significantly greater than that observed in the W-AJS group ($[F(1,13)=7.89]$; $P<0.007$) and both CON groups ($[F(1,11)>12.01]$; $P<0.0007$). The average Δ HR for the W-AJS group was also significantly greater than the average Δ HR over 20 min of both CON groups ($[F(1,11)>5.55]$; $P<0.01$). The CON groups did not exhibit any noticeable Δ HR during the experiment and there was no significant difference between the strains $[F(1,9)=0.27]$. During the recovery period, there was no significant difference in the average Δ HR between all four groups.

Changes in FLI and CRH staining in the amygdala following AJS

Visual representation of three subnuclei along the rostral-caudal extent of the amygdala evaluated is shown in Figure 3A. As shown in Figures 3B-D, in general AJS induced a significant increase in FLI changes in all three subnuclei of the amygdala. Statistical analysis of changes in FLI in both the MEA and BLA did not identify any strain effect in the rostral, middle, or caudal divisions $[F(3,23)<1.4]$, however, there was a significant treatment effect in the caudal (Fig. 3B&C), middle, and rostral divisions ($[F(1,23)>25.21]$; $P<0.001$; see Table 1). Similarly, in the caudal (Figure 3D, left panel) and middle CEA (Table 1) only a significant treatment effect was identified $[F(1,23)>5.26]$. In the rostral CEA (Figure 3D, right panel) however, both a significant treatment effect (AJS induced a significant increase in FLI above CON; $[F(1,23)=30.56]$; $P<0.001$) and a significant strain effect ($[F(1,23)=5.14]$; $P<0.03$) were identified. The strain effect in the rostral CEA was associated with a lower level of FLI in the SHR versus the Wistars overall.

In addition to changes in FLI, AJS also induced a significant increase in the number of CRH-positive neurons in the caudal and middle CEA in both strains ($[F(1,23)>7.41]$; $P<0.01$; Figure 4). In general, the number of CRH-positive neurons was greater in the SHR following AJS compared to the Wistar, however, statistical analysis only identified a significant effect of strain in the caudal CEA ($[F(1,23)=8.72]$; $P<0.008$).

Changes in FLI in LC and the hypothalamus following AJS

Figure 5A depicts the typical pattern of FLI cells observed in the rostral LC of a SHR and Wistar following AJS. AJS induced a significant increase in FLI in both the rostral and caudal LC relative to CON ($[F(1,23)>36.13]$; $P<0.0001$). In the caudal LC, there was no effect of strain on FLI ($[F(1,23)=1.78]$; $P>0.2$) following AJS. In the rostral LC, however, there was a significant interaction between strain and treatment $[F(3,23)=12.04]$. Further analysis identified that there was a greater increase in FLI in the rostral LC in the SHR-AJS group compared to the W-AJS, SHR-CON, and W-CON groups ($[F(1,11)>23.4]$; $P<0.001$).

FLI in the W-AJS group was also significantly greater than FLI in the W-CON and SHR-CON groups ($[F(1,11)] > 32.07$; $P < 0.001$). No significant difference in FLI between strains was observed between the CON groups ($[F(1,9)] = 0.11$; $P > 0.7$).

Figure 6 illustrates the effect of AJS on FLI levels in the hypothalamus. In all regions analyzed, a significant effect of treatment on FLI was identified [$F(1,23) > 14.37$], but no significant strain differences were found [$F(1,23) < 1.69$]. For example, in both the magnocellular and parvocellular regions of the PVN, AJS induced a significant increase in FLI compared to CON groups [$F(1,23) = 14.37$] and [$F(1,23) = 24.36$]; $P < 0.0001$, respectively; Fig. 6A). In the DMH and the ARC, there was also a significant increase in FLI in the AJS groups compared to the CON groups (Fig. 6B, [$F(1,23) = 57.29$] and [$F(1,23) = 26.36$], respectively; $P < 0.0001$).

DISCUSSION

The present study was undertaken to identify for the first time differences in the response pattern of neurons in the amygdala following exposure to an acute stressor in the SHR versus a normotensive control. Three new findings were identified. First, AJS induced significant increases in FLI along the rostral-caudal extent of all three subnuclei of the amygdala evaluated in both the SHR and Wistar rats compared to controls. Contrary to our original hypothesis, however, the only strain-related difference in FLI was localized to the rostral CEA and in this instance FLI was significantly lower in the SHR versus the Wistar. Furthermore, no strain-related differences were identified in the MEA as originally hypothesized. Second, our results identified for the first time that the number of CRH-positive cells in the CEA were significantly greater in the SHR compared to the Wistar and this difference was localized to the caudal CEA. Finally, associated with the very select changes in both FLI and CRH staining in the CEA of the SHR, we identified a parallel increase in FLI in the rostral LC that was significantly greater in the SHR following AJS. This association between altered neuronal patterning in the CEA and LC of the SHR is intriguing since there is a well characterized anatomical interconnection between CRH neurons in the CEA and neurons in the rostral pole of the LC that has been proposed to be involved in the stress response (69,70). Coupled with the exaggerated cardiovascular response to acute stress observed in the SHR, these results raise the new possibility that stress-related autonomic dysregulation in hypertension may involve abnormal regulation of CRH-positive neurons in the CEA with descending interconnections to the rostral LC (10,35).

Cardiovascular response during AJS exposure in the SHR

In the present study, we used a model of AJS that did not involve restraint. This model was developed based on recent evidence suggesting that patterns of brain activation, particularly in the amygdala, are dependent on the type of stressor applied, either psychological or physical (15,24). Most AJS models previously used to evaluate the stress response in the SHR compared to normotensive strains have utilized some method of restraint while exposing the animals to AJS. Since restraint is likely to be interpreted as a form of physical stress, those methods may have potentially complicated the results by testing multiple forms of stressful stimuli simultaneously (21,24,46). We also conditioned the rats to the air noise component of AJS prior to testing to prevent any added effects induced by audiogenic stress (46,49). With the former precautions, the SHR responded to the AJS with a greater elevation in MAP and HR from baseline compared to the Wistar. Other stressors applied to the SHR, such as noise and alerting stimuli, have also been shown to elicit cardiovascular responses comparable to those generated by our AJS model (31,52) suggesting that our results primarily reflect an exaggerated response to an acute psychological stressor, similar to what

one might experience when suddenly frightened by an acute, novel or threatening stimulus such as speaking in public for the first time or during a near-miss vehicle collision.

FLI in the amygdala following AJS in the SHR

Based on previous lesion work (24), in the present study it was hypothesized that AJS would induce a different pattern of FLI in the CEA of the SHR compared to the Wistar rat. Accordingly, AJS elicited significant increases in FLI in both the SHR and Wistar along the caudal-rostral extent of the CEA and a strain-related difference was identified in the rostral CEA. Somewhat unexpected however, this strain-related difference in FLI included a significantly lower number of FLI neurons in the SHR versus Wistar. Since previous reports suggest that FLI in the CEA increases in response to elevations in MAP (9,41), it is unlikely that this difference between strains in the rostral CEA is related to differences in pressure-related feedback (ie., baroreceptor afferent input) to the amygdala. Alternatively, our observation raises the possibility that the exaggerated autonomic stress response in the SHR may be related to a change in the overall balance of excitation/inhibition within the CEA during stress. For example, several studies have demonstrated that psychological stressors can actually reduce FLI levels in the CEA, while physical stressors generate the opposite response (16,32,56). Indeed, when baseline levels of FLI are elevated by amphetamine administration the addition of an external stressor has been reported to reduce FLI in the CEA (15). Accordingly, it has been proposed that activation of the inhibitory interneurons within other subnuclei of the amygdala (ie., BLA (40)) by fearful or stressful stimuli may act to inhibit CEA inhibitory projection neurons thereby disinhibiting distal target sites (51,53). Unfortunately, the neurochemical content of neurons activated by AJS projecting to the CEA were not characterized in the present study, but our results raise the possibility that GABAergic inhibition in the CEA may be exaggerated in the SHR and this elevated inhibition, specifically in the rostral CEA, contributes to the exaggerated stress response observed in hypertension, possibly via elevated disinhibition of autonomic control nuclei.

In addition to dysregulation of the CEA, we had hypothesized that AJS would induce a different pattern of FLI in MEA of the SHR compared to the Wistar. This hypothesis was based on data which have demonstrated both a reduction in baseline blood pressure following destruction of the MEA in the SHR (23) and attenuation of the cardiovascular response to restraint stress following chemical blockade of the MEA (39). Furthermore, activation of the MEA in response to stress has been linked to hormone release and there is evidence that the HPA axis may be dysregulated in the SHR (17,18,29). Yet, in the present study no strain-related differences in FLI were observed in the MEA of the SHR versus the Wistar following AJS exposure. Indeed, the pattern of FLI induced in the MEA of the SHR in response to AJS was similar in magnitude to that previously reported following psychological stress exposure for two normotensive strains, the Spague Dawley and Wistar rats (16,17). Thus, despite evidence of the MEA's possible role in stress, the results of the present study do not implicate the MEA (or the BLA) in playing a unique role in the exaggerated cardiovascular response to stress typically observed in the SHR.

CRH labeling in the CEA following AJS in the SHR

The only prior evidence regarding dysregulation of neuronal CRH levels in the SHR has been localized to the PVN. Previous investigators have identified that basal CRH mRNA levels in the PVN of the SHR are either lower or not different compared to a normotensive strain (28,30). During restraint, however, CRH mRNA expression in the PVN has been shown to increase more in the SHR compared to normotensive controls (38). Increased expression of CRH in the PVN in response to acute stress has been hypothesized to be related to the altered regulation of HPA axis implicated in the SHR (29). The present study is the first to evaluate CRH protein levels in the amygdala of the SHR and the results

demonstrate that similar to the PVN, CRH expression in the CEA is significantly elevated in response to AJS and neuronal CRH expression is greater in the caudal CEA of the SHR compared to the Wistar strain. Although there is strong evidence that modulation of CRH expression in the amygdala can occur in response to acute stress (33) and is critical for both the behavioral expression of fear (33,37) and autonomic responses to both stressful (72) and non-stressful stimuli (73), additional studies are needed to fully evaluate how stress-induced changes in CRH protein expression in the CEA contribute to the exaggerated autonomic response to stress reported here in the SHR.

FLI in the locus coeruleus following AJS

CRH neuronal activity in the CEA has been implicated in regulating output from the CEA to the brainstem (6) and there is evidence that descending input from CEA-CRH neurons to the LC mediates stress-related excitation of LC area neurons in normotensive animals (12,13,70). Furthermore, CRH microinjected into the LC has been reported to increase neuronal discharge and cortical norepinephrine release (61,68). The LC core has a dense population of noradrenergic neurons that either project rostrally to the forebrain or caudally to the spinal cord (45,55). Lesion and microinjection studies have demonstrated that the caudal portion of the LC is active during hypotension. The rostral component appears to be primarily active during psychological stress (3,8), but is not activated by peripherally-induced increases in blood pressure (9,41). In the present study, the rostral LC demonstrated a marked increase in FLI in the SHR-AJS group that was significantly greater than that induced in the W-AJS or both CON groups. The increased FLI in the rostral LC of SHR that we observed in response to AJS suggests that hyper-arousal of the LC, leading to increased noradrenergic release in the forebrain (7,48), may also play an important role in the exaggerated stress-like behaviors associated with hypertension.

There are acknowledged alterations in both the anatomy and activity of LC neurons in the SHR, including reduced basal neuronal discharge, decreased α -2 adrenergic receptor sensitivity (19,20,47), and reduced GABAergic secretion following intravenous infusion of norepinephrine (35,60). In one previous study, only modest increases in FLI in the LC were identified following air puff stress in the SHR compared to another normotensive control, the WKY rat (50). In that study, however, single puffs of air were used to induce stress, compared to the 20 min of continuous AJS used in the present study, thus the difference in the intensity of the stress between studies may explain the more robust difference in neuronal activation within the rostral LC exhibited in the SHR versus the Wistar in the present study. Together, the increase in CRH expression in the CEA and FLI in the rostral LC in our study suggest that the relationship between these two brain regions may be critically linked to the exaggerated cardiovascular reactivity in the SHR during stress.

FLI in hypothalamic structures following AJS

Finally, the pattern of FLI in three hypothalamic regions known to be involved in stress-related responses, the DMH, ARC, and PVN was evaluated (67). Interestingly, similar increases in FLI in both the Wistar and SHR were observed following AJS. Since all three hypothalamic subnuclei have been implicated in mediating autonomic responses to stress, and the response to AJS was exaggerated in the SHR, it was unexpected that similar changes in FLI would be observed in both the Wistar and the SHR (22,50,63,64). Moreover, several previous studies have demonstrated significant increases in FLI in the hypothalamus and the brainstem in response to AJS combined with restraint in the SHR when compared to another normotensive strain, the Wistar-Kyoto (WKY) rat (34,38,50). Thus, results of the present study suggest that the capacity for neuronal activation in the hypothalamus during AJS in the absence of physical restraint may be relatively normal in the SHR when compared to a different normotensive strain. Indeed, one methodological consideration to be taken into

account in the interpretation of the present results is the fact that the majority of previous studies investigating the impact of stress on regional brain activation in the SHR have utilized the WKY as a normotensive control (11,15,66). In the present study, we chose to use the Wistar as a control, over the traditional WKY, based on evidence that the WKY strain may be hypo-responsive to stressful stimuli compared to other normotensive strains (5,12).

Conclusion

The results of the current study provide new information regarding the role of the amygdala in the SHR following exposure to novel unrestrained AJS. Of the three subnuclei of the amygdala analyzed only the CEA demonstrated strain-related differences. Strain-effects included a greater increase in CRH labeling in the caudal CEA of the SHR compared to the Wistar rat that was coupled to significantly lower levels of FLI in the rostral CEA of the SHR. Local application of CRH in the CEA has been shown to elicit tachycardia and has been hypothesized to involve local inhibitory pathways (73), thus these two observations suggest that the exaggerated autonomic response to stress typically observed in the SHR may be related to both elevated CRH release, either locally or to efferent projection sites, and an exaggerated local inhibition which may be linked to disinhibition of descending or ascending autonomic control regions. Parallel to these strain specific changes in the CEA, we also identified an elevation of FLI in the rostral LC in the SHR compared to the Wistar after AJS. Since CRH containing CEA neurons target the rostral LC, this observation raises the possibility that the exaggerated autonomic response stress in the SHR may also be linked to dysregulation of CRH input from the CEA to the rostral LC. These observations provide a possible target for future investigations into the treatment for exaggerated stress responses in hypertension.

Acknowledgments

The authors thank Ms. Mabelin Castellanos for her technical help on this project and the American Heart Association-Florida/Puerto Rico Affiliate (KP) and NIH (LH) for their research support.

REFERENCES

1. al'Absi M, Lovallo WR, McKey BS, Pincomb GA. Borderline hypertensives produce exaggerated adrenocortical responses to mental stress. *Psychosom Med.* 1994; 56:245–250. [PubMed: 8084971]
2. Angrilli A, Mauri A, Palomba D, Flor H, Birbaumer N, Sartori G, di Paola F. Startle reflex and emotion modulation impairment after a right amygdala lesion. *Brain.* 1996; 119(Pt 6):1991–2000. [PubMed: 9010003]
3. Anselmo-Franci JA, Peres-Polon VL, da Rocha-Barros VM, Moreira ER, Franci CR, Rocha MJ. C-fos expression and electrolytic lesions studies reveal activation of the posterior region of locus coeruleus during hemorrhage induced hypotension. *Brain Res.* 1998; 799:278–284. [PubMed: 9675311]
4. Asan E, Yilmazer-Hanke DM, Eliava M, Hantsch M, Lesch KP, Schmitt A. The corticotropin-releasing factor (CRF)-system and monoaminergic afferents in the central amygdala: investigations in different mouse strains and comparison with the rat. *Neuroscience.* 2005; 131:953–967. [PubMed: 15749348]
5. Bilanz-Bleuel A, Rech J, De Carli S, Holsboer F, Reul JM. Forced swimming evokes a biphasic response in CREB phosphorylation in extrahypothalamic limbic and neocortical brain structures in the rat. *Eur J Neurosci.* 2002; 15:1048–1060. [PubMed: 11918664]
6. Bohus B, Koolhaas JM, Luiten PG, Korte SM, Roozendaal B, Wiersma A. The neurobiology of the central nucleus of the amygdala in relation to neuroendocrine and autonomic outflow. *Prog Brain Res.* 1996; 107:447–460. [PubMed: 8782536]

7. Buffalari DM, Grace AA. Noradrenergic modulation of basolateral amygdala neuronal activity: opposing influences of alpha-2 and beta receptor activation. *J Neurosci.* 2007; 27:12358–12366. [PubMed: 17989300]
8. Carlson DE, Gann DS. Response of plasma adrenocorticotropin to injections of L-glutamate or norepinephrine in the dorsal rostral pons of cats. *Endocrinology.* 1991; 128:3021–3031. [PubMed: 1674687]
9. Chan R, Sawchenko PE. Spatially and temporally differentiated patterns of c-fos in brainstem catecholaminergic cell groups induced by cardiovascular challenges in the rat. *J Comp Neurol.* 1994; 348:433–460. [PubMed: 7844257]
10. Conti LH, Youngblood KL, Printz MP, Foote SL. Locus coeruleus electrophysiological activity and responsivity to corticotropin-releasing factor in inbred hypertensive and normotensive rats. *Brain Res.* 1997; 774:27–34. [PubMed: 9452188]
11. Cullinan WE, Herman JP, Battaglia DF, Akil H, Watson SJ. Pattern and time course of immediate early gene expression in rat brain following acute stress. *Neuroscience.* 1995; 64:477–505. [PubMed: 7700534]
12. Curtis AL, Bello NT, Connolly KR, Valentino RJ. Corticotropin-releasing factor neurones of the central nucleus of the amygdala mediate locus coeruleus activation by cardiovascular stress. *J Neuroendocrinol.* 2002; 14:667–682. [PubMed: 12153469]
13. Curtis AL, Bello NT, Valentino RJ. Evidence for functional release of endogenous opioids in the locus ceruleus during stress termination. *J Neurosci.* 2001; 21:RC152. [PubMed: 11406637]
14. Da Costa Gomez TM, Chandler SD, Behbehani MM. The role of the basolateral nucleus of the amygdala in the pathway between the amygdala and the midbrain periaqueductal gray in the rat. *Neurosci Lett.* 1996; 214:5–8. [PubMed: 8873118]
15. Day HE, Nebel S, Sasse S, Campeau S. Inhibition of the central extended amygdala by loud noise and restraint stress. *Eur J Neurosci.* 2005; 21:441–454. [PubMed: 15673443]
16. Dayas CV, Buller KM, Crane JW, Xu Y, Day TA. Stressor categorization: acute physical and psychological stressors elicit distinctive recruitment patterns in the amygdala and in medullary noradrenergic cell groups. *Eur J Neurosci.* 2001; 14:1143–1152. [PubMed: 11683906]
17. Dayas CV, Buller KM, Day TA. Neuroendocrine responses to an emotional stressor: evidence for involvement of the medial but not the central amygdala. *Eur J Neurosci.* 1999; 11:2312–2322. [PubMed: 10383620]
18. Dayas CV, Day TA. Opposing roles for medial and central amygdala in the initiation of noradrenergic cell responses to a psychological stressor. *Eur J Neurosci.* 2002; 15:1712–1718. [PubMed: 12059979]
19. Engberg G, Orelund L, Thoren P, Svensson T. Locus coeruleus neurons show reduced alpha 2-receptor responsiveness and decreased basal activity in spontaneously hypertensive rats. *J Neural Transm.* 1987; 69:71–83. [PubMed: 3035085]
20. Felten DL, Rubin LR, Felten SY, Weyhenmeyer JA. Anatomical alterations in locus coeruleus neurons in the adult spontaneously hypertensive rat. *Brain Res Bull.* 1984; 13:433–436. [PubMed: 6498539]
21. Folkow B, Hallback-Nordlander M, Martner J, Nordborg C. Influence of amygdala lesions on cardiovascular responses to alerting stimuli, on behaviour and on blood pressure development in spontaneously hypertensive rats. *Acta Physiol Scand.* 1982; 116:133–139. [PubMed: 7168349]
22. Fontes MA, Tagawa T, Polson JW, Cavanagh SJ, Dampney RA. Descending pathways mediating cardiovascular response from dorsomedial hypothalamic nucleus. *Am J Physiol Heart Circ Physiol.* 2001; 280:H2891–2901. [PubMed: 11356650]
23. Fukumori R, Nishigori Y, Goshima Y, Kubo T. Contribution of the medial amygdaloid nucleus to the development of hypertension in spontaneously hypertensive rats. *Neurosci Lett.* 2004; 365:128–131. [PubMed: 15245793]
24. Galeno TM, Van Hoesen GW, Brody MJ. Central amygdaloid nucleus lesion attenuates exaggerated hemodynamic responses to noise stress in the spontaneously hypertensive rat. *Brain Res.* 1984; 291:249–259. [PubMed: 6697190]

25. Gianaros PJ, Sheu LK, Matthews KA, Jennings JR, Manuck SB, Hariri AR. Individual differences in stressor-evoked blood pressure reactivity vary with activation, volume, and functional connectivity of the amygdala. *J Neurosci*. 2008; 28:990–999. [PubMed: 18216206]
26. Gray TS, Carney ME, Magnuson DJ. Direct projections from the central amygdaloid nucleus to the hypothalamic paraventricular nucleus: possible role in stress-induced adrenocorticotropin release. *Neuroendocrinology*. 1989; 50:433–446. [PubMed: 2554178]
27. Hallback M, Folkow B. Cardiovascular responses to acute mental ‘stress’ in spontaneously hypertensive rats. *Acta Physiol Scand*. 1974; 90:684–698. [PubMed: 4857612]
28. Hashimoto K, Hattori T, Murakami K, Suemaru S, Kawada Y, Kageyama J, Ota Z. Reduction in brain immunoreactive corticotropin-releasing factor (CRF) in spontaneously hypertensive rats. *Life Sci*. 1985; 36:643–647. [PubMed: 3871498]
29. Hashimoto K, Makino S, Hirasawa R, Takao T, Sugawara M, Murakami K, Ono K, Ota Z. Abnormalities in the hypothalamo-pituitary-adrenal axis in spontaneously hypertensive rats during development of hypertension. *Endocrinology*. 1989; 125:1161–1167. [PubMed: 2547578]
30. Hattori T, Hashimoto K, Ota Z. Brain corticotropin releasing factor in the spontaneously hypertensive rat. *Hypertension*. 1986; 8:1027–1031. [PubMed: 3490439]
31. Hayward LF, Johnson AK, Felder RB. Arterial chemoreflex in conscious normotensive and hypertensive adult rats. *Am J Physiol*. 1999; 276:H1215–1222. [PubMed: 10199845]
32. Helfferich F, Palkovits M. Acute audiogenic stress-induced activation of CRH neurons in the hypothalamic paraventricular nucleus and catecholaminergic neurons in the medulla oblongata. *Brain Res*. 2003; 975:1–9. [PubMed: 12763588]
33. Hsu DT, Chen FL, Takahashi LK, Kalin NH. Rapid stress-induced elevations in corticotropin-releasing hormone mRNA in rat central amygdala nucleus and hypothalamic paraventricular nucleus: an in situ hybridization analysis. *Brain Res*. 1998; 788:305–310. [PubMed: 9555067]
34. Imaki T, Naruse M, Harada S, Chikada N, Nakajima K, Yoshimoto T, Demura H. Stress-induced changes of gene expression in the paraventricular nucleus are enhanced in spontaneously hypertensive rats. *J Neuroendocrinol*. 1998; 10:635–643. [PubMed: 9725716]
35. Kaehler ST, Salchner P, Singewald N, Philippu A. Differential amino acid transmission in the locus coeruleus of Wistar Kyoto and spontaneously hypertensive rats. *Naunyn Schmiedeberg Arch Pharmacol*. 2004; 370:381–387. [PubMed: 15526108]
36. Knardahl S, Hendley ED. Association between cardiovascular reactivity to stress and hypertension or behavior. *Am J Physiol*. 1990; 259:H248–257. [PubMed: 1973873]
37. Kolber BJ, Roberts MS, Howell MP, Wozniak DF, Sands MS, Muglia LJ. Central amygdala glucocorticoid receptor action promotes fear-associated CRH activation and conditioning. *Proc Natl Acad Sci U S A*. 2008; 105:12004–12009. [PubMed: 18695245]
38. Krukoff TL, MacTavish D, Jhamandas JH. Hypertensive rats exhibit heightened expression of corticotropin-releasing factor in activated central neurons in response to restraint stress. *Brain Res Mol Brain Res*. 1999; 65:70–79. [PubMed: 10036309]
39. Kubo T, Okatani H, Nishigori Y, Hagiwara Y, Fukumori R, Goshima Y. Involvement of the medial amygdaloid nucleus in restraint stress-induced pressor responses in rats. *Neurosci Lett*. 2004; 354:84–86. [PubMed: 14698487]
40. LeDoux J. The amygdala. *Curr Biol*. 2007; 17:R868–874. [PubMed: 17956742]
41. Li Y, Dampney RA. Expression of Fos-like protein in brain following sustained hypertension and hypotension in conscious rabbits. *Neuroscience*. 1994; 61:613–634. [PubMed: 7969933]
42. Ma S, Morilak DA. Norepinephrine release in medial amygdala facilitates activation of the hypothalamic-pituitary-adrenal axis in response to acute immobilisation stress. *J Neuroendocrinol*. 2005; 17:22–28. [PubMed: 15720472]
43. Makino S, Shibasaki T, Yamauchi N, Nishioka T, Mimoto T, Wakabayashi I, Gold PW, Hashimoto K. Psychological stress increased corticotropin-releasing hormone mRNA and content in the central nucleus of the amygdala but not in the hypothalamic paraventricular nucleus in the rat. *Brain Res*. 1999; 850:136–143. [PubMed: 10629757]
44. Marchant N, Densmore VS, Osborne PB. Co-expression of prodynorphin and corticotropin-releasing hormone in the rat central amygdala: Evidence of two distinct endogenous opioid systems in the lateral division. *J Comp Neurol*. 2007; 504:702–715. [PubMed: 17722034]

45. Mason ST, Fibiger HC. Regional topography within noradrenergic locus coeruleus as revealed by retrograde transport of horseradish peroxidase. *J Comp Neurol*. 1979; 187:703–724. [PubMed: 90684]
46. McDougall SJ, Lawrence AJ, Widdop RE. Differential cardiovascular responses to stressors in hypertensive and normotensive rats. *Exp Physiol*. 2005; 90:141–150. [PubMed: 15542615]
47. Olpe HR, Berecek KH, Jones RS, Steinmann MW, Sonnenburg C, Hofbauer KG. Reduced activity of locus coeruleus neurons in hypertensive rats. *J Hypertens Suppl*. 1985; 3:S93–95. [PubMed: 3913758]
48. Palkovits M, Baffi JS, Pacak K. The role of ascending neuronal pathways in stress-induced release of noradrenaline in the hypothalamic paraventricular nucleus of rats. *J Neuroendocrinol*. 1999; 11:529–539. [PubMed: 10444310]
49. Palmer AA, Printz MP. Differences between SHR and WKY following the airpuff startle stimulus in the number of Fos expressing, RVLN projecting neurons. *Clin Exp Hypertens*. 2002; 24:125–139. [PubMed: 11883788]
50. Palmer AA, Printz MP. Strain differences in Fos expression following airpuff startle in Spontaneously Hypertensive and Wistar Kyoto rats. *Neuroscience*. 1999; 89:965–978. [PubMed: 10199628]
51. Pape HC. GABAergic neurons: gate masters of the amygdala, mastered by dopamine. *Neuron*. 2005; 48:877–879. [PubMed: 16364892]
52. Pardon MC, Gould GG, Garcia A, Phillips L, Cook MC, Miller SA, Mason PA, Morilak DA. Stress reactivity of the brain noradrenergic system in three rat strains differing in their neuroendocrine and behavioral responses to stress: implications for susceptibility to stress-related neuropsychiatric disorders. *Neuroscience*. 2002; 115:229–242. [PubMed: 12401336]
53. Pare D, Royer S, Smith Y, Lang EJ. Contextual inhibitory gating of impulse traffic in the intra-amygdaloid network. *Ann N Y Acad Sci*. 2003; 985:78–91. [PubMed: 12724150]
54. Paxinos, G.; Watson, C. *The Rat Brain in Stereotaxic Coordinates*. 1998.
55. Proudfit HK, Clark FM. The projections of locus coeruleus neurons to the spinal cord. *Prog Brain Res*. 1991; 88:123–141. [PubMed: 1813919]
56. Rotllant D, Nadal R, Armario A. Differential effects of stress and amphetamine administration on Fos-like protein expression in corticotropin releasing factor-neurons of the rat brain. *Dev Neurobiol*. 2007; 67:702–714. [PubMed: 17443818]
57. Saha S. Role of the central nucleus of the amygdala in the control of blood pressure: descending pathways to medullary cardiovascular nuclei. *Clin Exp Pharmacol Physiol*. 2005; 32:450–456. [PubMed: 15854157]
58. Sajdyk TJ, Schober DA, Gehlert DR, Shekhar A. Role of corticotropin-releasing factor and urocortin within the basolateral amygdala of rats in anxiety and panic responses. *Behav Brain Res*. 1999; 100:207–215. [PubMed: 10212068]
59. Shekhar A, Sajdyk TJ, Gehlert DR, Rainnie DG. The amygdala, panic disorder, and cardiovascular responses. *Ann N Y Acad Sci*. 2003; 985:308–325. [PubMed: 12724167]
60. Singewald N, Schneider C, Philippu A. Disturbances in blood pressure homeostasis modify GABA release in the locus coeruleus. *Neuroreport*. 1994; 5:1709–1712. [PubMed: 7827313]
61. Smagin GN, Swiergiel AH, Dunn AJ. Corticotropin-releasing factor administered into the locus coeruleus, but not the parabrachial nucleus, stimulates norepinephrine release in the prefrontal cortex. *Brain Res Bull*. 1995; 36:71–76. [PubMed: 7882052]
62. Stein MB, Simmons AN, Feinstein JS, Paulus MP. Increased amygdala and insula activation during emotion processing in anxiety-prone subjects. *Am J Psychiatry*. 2007; 164:318–327. [PubMed: 17267796]
63. Stotz-Potter EH, Morin SM, DiMicco JA. Effect of microinjection of muscimol into the dorsomedial or paraventricular hypothalamic nucleus on air stress-induced neuroendocrine and cardiovascular changes in rats. *Brain Res*. 1996; 742:219–224. [PubMed: 9117398]
64. Stotz-Potter EH, Willis LR, DiMicco JA. Muscimol acts in dorsomedial but not paraventricular hypothalamic nucleus to suppress cardiovascular effects of stress. *J Neurosci*. 1996; 16:1173–1179. [PubMed: 8558246]

65. Swiergiel AH, Takahashi LK, Kalin NH. Attenuation of stress-induced behavior by antagonism of corticotropin-releasing factor receptors in the central amygdala in the rat. *Brain Res.* 1993; 623:229–234. [PubMed: 8221104]
66. Trneckova L, Rotllant D, Klenerova V, Hynie S, Armario A. Dynamics of immediate early gene and neuropeptide gene response to prolonged immobilization stress: evidence against a critical role of the termination of exposure to the stressor. *J Neurochem.* 2007; 100:905–914. [PubMed: 17217423]
67. Tsigos C, Chrousos GP. Hypothalamic-pituitary-adrenal axis, neuroendocrine factors and stress. *J Psychosom Res.* 2002; 53:865–871. [PubMed: 12377295]
68. Valentino RJ, Foote SL, Aston-Jones G. Corticotropin-releasing factor activates noradrenergic neurons of the locus coeruleus. *Brain Res.* 1983; 270:363–367. [PubMed: 6603889]
69. Van Bockstaele E, Bajic D, Proudfit H, Valentino R. Topographic architecture of stress-related pathways targeting the noradrenergic locus coeruleus. *Physiol Behav.* 2001; 73:273–283. [PubMed: 11438352]
70. Van Bockstaele EJ, Colago EE, Valentino RJ. Amygdaloid corticotropin-releasing factor targets locus coeruleus dendrites: substrate for the co-ordination of emotional and cognitive limbs of the stress response. *J Neuroendocrinol.* 1998; 10:743–757. [PubMed: 9792326]
71. Veening JG, Swanson LW, Sawchenko PE. The organization of projections from the central nucleus of the amygdala to brainstem sites involved in central autonomic regulation: a combined retrograde transport-immunohistochemical study. *Brain Res.* 1984; 303:337–357. [PubMed: 6204716]
72. Watanabe M, Kucenas S, Bowman TA, Ruhlman M, Knuepfer MM. Angiotensin II and CRF receptors in the central nucleus of the amygdala mediate hemodynamic response variability to cocaine in conscious rats. *Brain Res.* 2010; 1309:53–65. [PubMed: 19879859]
73. Wiersma A, Bohus B, Koolhaas JM. Corticotropin-releasing hormone microinfusion in the central amygdala diminishes a cardiac parasympathetic outflow under stress-free conditions. *Brain Res.* 1993; 625:219–227. [PubMed: 8275304]
74. Zald DH. The human amygdala and the emotional evaluation of sensory stimuli. *Brain Res Brain Res Rev.* 2003; 41:88–123. [PubMed: 12505650]

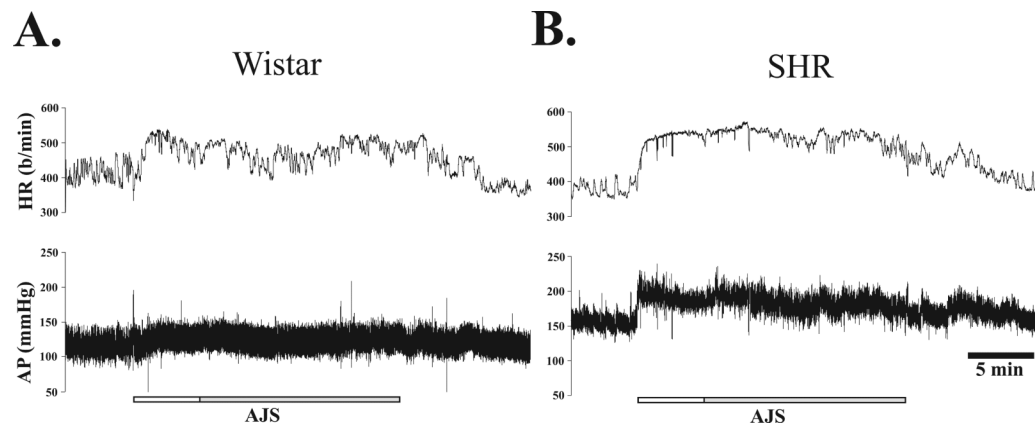


Figure 1. Recording of arterial pressure (AP) and heart rate (HR) from a single unrestrained male Wistar (A) and SHR (B) rat before, during, and immediately following exposure to unrestrained AJS

Gray and white horizontal bar represents the 20 min duration of air jet stress (AJS), including an initial 5 min of randomly directed AJS (white) and 15 min of sustained AJS in which the direction of air changes in 1 min intervals (gray). The total recording represents 35 min.

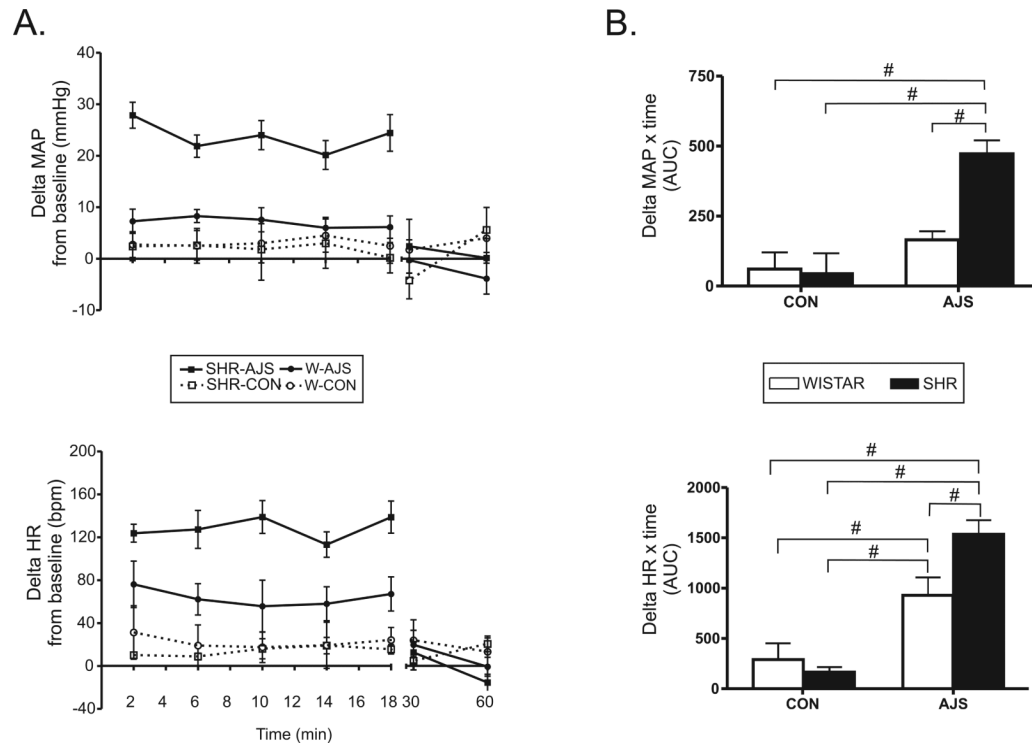


Figure 2. Change from baseline for mean arterial pressure (MAP) and heart rate (HR) in response to air jet stress (AJS) or noise control (CON) between SHR and Wistar rats
 A. Two min averages of Δ MAP and Δ HR for each group during (20 min) and after (30 and 60 min) the treatment period. W-CON (n=5), W-AJS (n=7), SHR-CON (n=5), and SHR-AJS (n=7). B. Area under the curve for Δ MAP and Δ HR during the treatment period. # indicates significance between individual strain and treatment groups identified (P<0.01). W=Wistar; SHR=Spontaneously hypertensive rat; AJS=air jet stress; CON=control group.

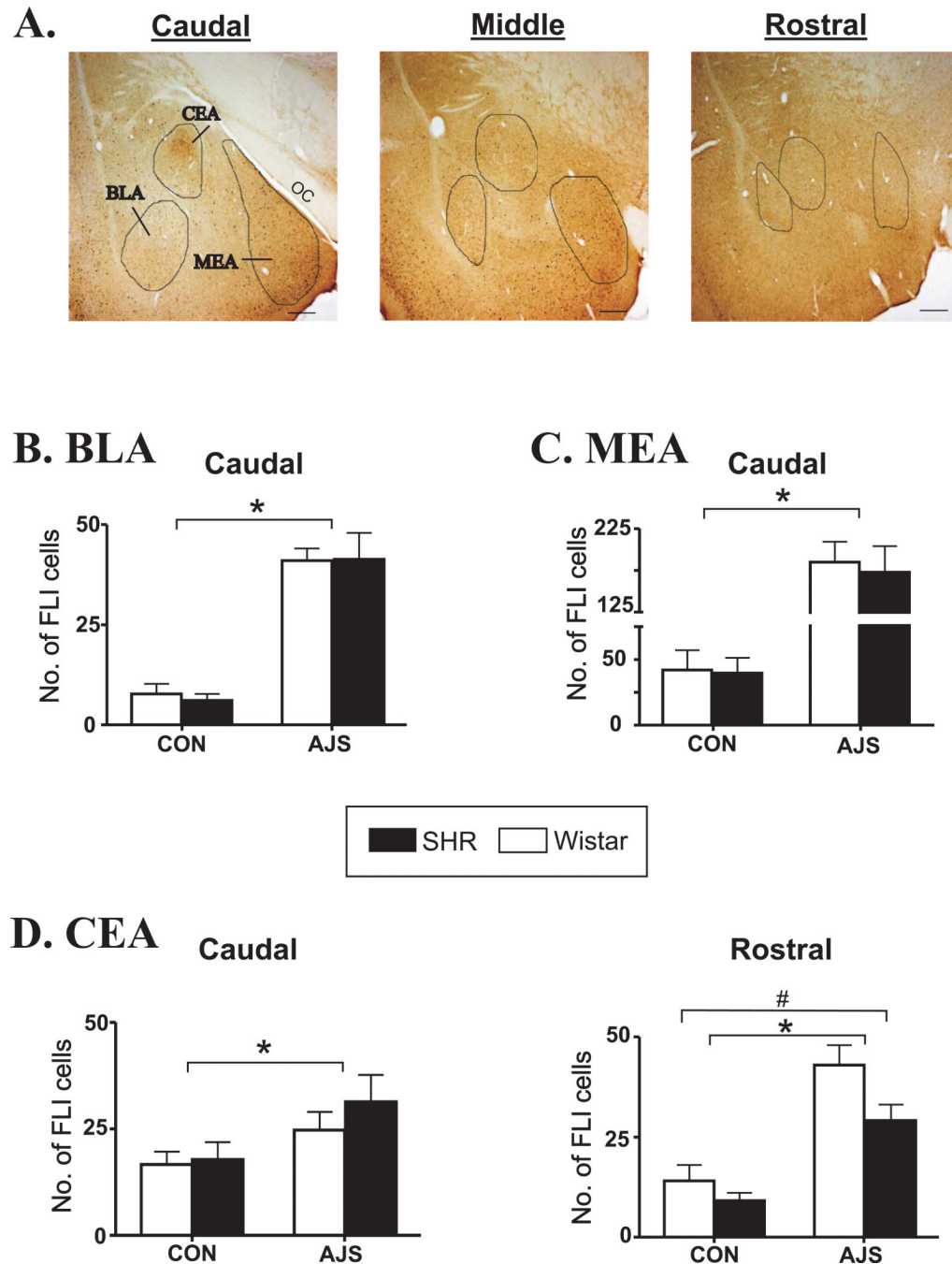
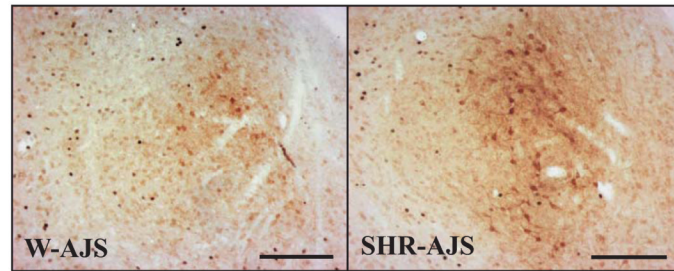


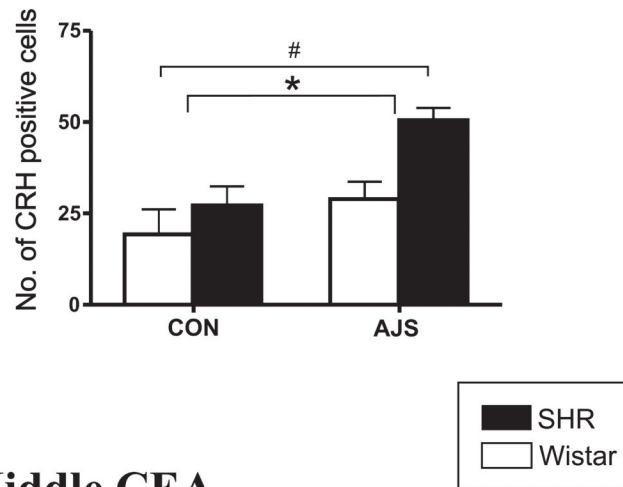
Figure 3. Increases in FLI in the central, basolateral, and medial subnuclei of the amygdala following AJS

A.) Visual representation of the caudal, middle, and rostral subdivisions of the amygdala evaluated from a single rat. Circular outlines define approximate location of each subnucleus. Black bar represents 50 μ m. B.) Average number of FLI-positive neurons in the caudal BLA. C.) Average number of FLI-positive cells in the caudal MEA. D.) Average number of FLI-positive neurons in the caudal and rostral CEA. *indicates significant treatment effect ($P<0.03$); # indicates significant strain effect ($P<0.03$). FLI=fos-like immunoreactivity; CEA=central nucleus of the amygdala; BLA=basolateral nucleus of the amygdala; MEA=medial nucleus of the amygdala; OC=optic tract.

A.



B. Caudal CEA



C. Middle CEA

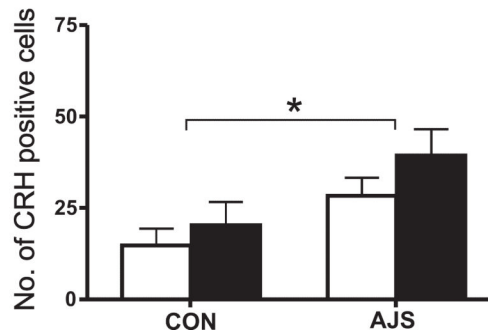
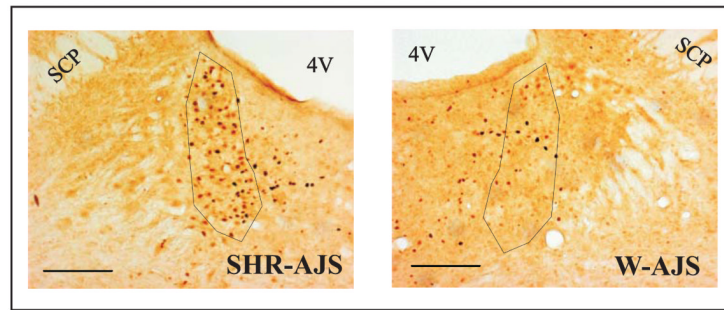
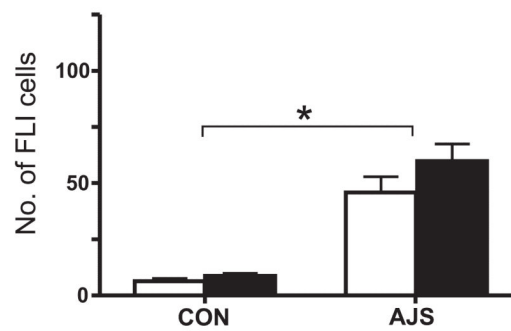


Figure 4. Increases in the number of CRH-positive cells in the CEA following AJS
 A.) CRH staining in the CEA representing both the W-AJS and SHR-AJS groups. Black bar represents 100 μ m. B.) Number of CRH-positive cells in the caudal CEA. C. Number of CRH-positive cells in the middle CEA. * indicates significant treatment effect ($P < 0.01$). # indicates significant strain effect ($P < 0.008$). CEA= central nucleus of the amygdala; CRH=corticotropin releasing hormone.

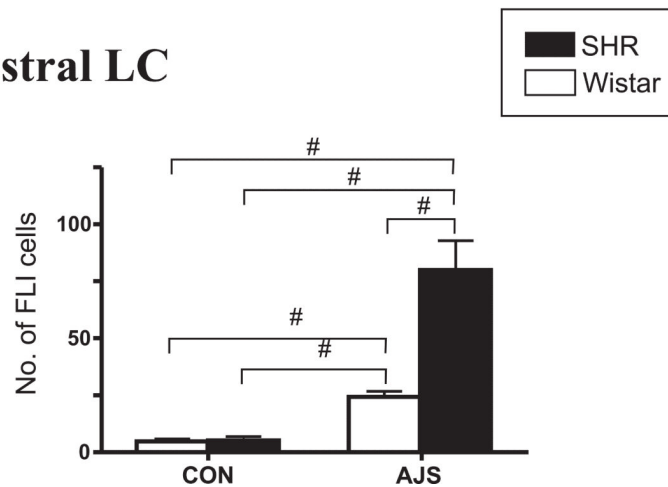
A.



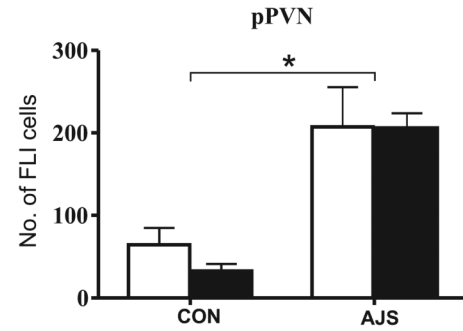
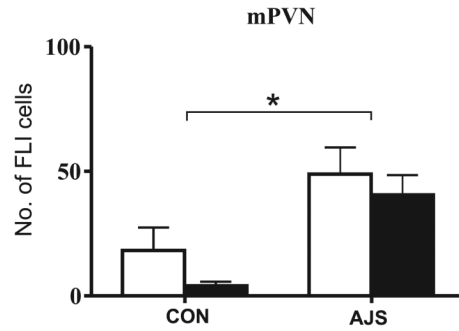
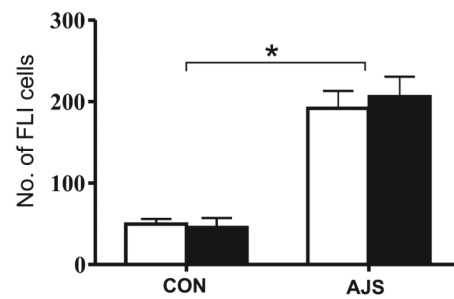
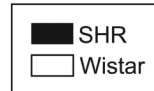
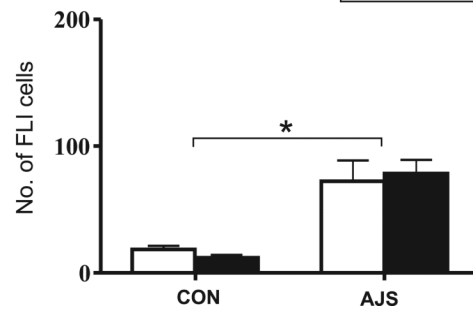
B. Caudal LC



C. Rostral LC

**Figure 5. Pattern of FLI in the locus coeruleus (LC) following AJS**

A.) Images of rostral LC from individual animals following AJS. Black bar represents 100 μ m. B.) Number of FLI in the caudal LC. C.) Number of FLI in the rostral LC. * $P < 0.007$ indicates significant treatment effect (both strains combined). # indicates significance between individual strain and treatment groups identified ($P < 0.001$). SCP=superior cerebellar peduncle; 4V=fourth ventricle.

A. PVN**B. DMH****C. Arcuate****Figure 6. Pattern of FLI in the hypothalamus following AJS**

A.) Number of FLI positive cells in magnocellular PVN (mPVN) and parvocellular PVN (pPVN). B.) Number of FLI positive cells in the DMH. C.) Number of FLI positive cells in the arcuate nucleus. * $P < 0.05$ indicates significance between treatment groups (both strains combined). PVN=paraventricular nucleus; DMH=dorsomedial hypothalamus.

Table 1

AVERAGE C-FOS COUNTS IN MIDDLE AND ROSTRAL DIVISIONS OF SELECT AMYGDALOID SUBNUCLEI FOLLOWING AIRJET STRESS VERSUS CONTROL TREATMENT

Location	WIS CON	SHR CON	WIS AJS	SHR AJS	Treatment effect
CEA					
Middle	13±1.5	16±6	30±4	31±3	P<0.001
Rostral [#]	15±4	9±2	43±5	29±4	P<0.0001
BLA					
Middle	4±1.6	4±1.7	38±5	30±4	P<0.001
Rostral	2±0.6	3±1	19±4	14±3	P<0.001
MEA					
Middle	31±10	24±9	165±15	138±22	P<0.001
Rostral	12±3	20±3	95±5	101±10	P<0.001

CEA indicates central nucleus of the amygdala; BLA indicates basolateral amygdala; MEA indicates medial amygdala. Treatment effect indicates airjet stress (AJS) counts were significantly different from control (CON) independent of strain.

[#] indicates significant strain effect (see Fig. 3 for more details) Data are mean±SEM